Electronic Supporting Information

Nd^{3+} doped $BiVO_4$ luminescent nanothermometers of high sensitivity

*Pascal M. Gschwend[1], Fabian H.L. Starsich[1], Robert C. Keitel[2], and Sotiris E. Pratsinis[1]**

[1] Particle Technology Laboratory, Institute of Process Engineering, Department of Mechanical and Process Engineering, ETH Zürich, Sonneggstrasse 3, CH-8092 Zurich, Switzerland

[2] Optical Materials Engineering Laboratory, Institute of Process Engineering, Department of Mechanical and Process Engineering, ETH Zürich, Leonhardstrasse 21, CH-8092 Zurich, Switzerland

*Corresponding author

Sotiris E. Pratsinis; Tel: +41 44 632 31 80; fax : +41 44 632 15 95 ; email : sotiris.pratsinis@ptl.mavt.ethz.ch

Date : 24.4.2019

ORCID

Pascal M. Gschwend: 0000-0002-5980-1959
Fabian H. L. Starsich: 0000-0003-0724-764X
Robert C. Keitel: 0000-0002-9412-8034
Sotiris E. Pratsinis: 0000-0003-2042-249X

Experimental

Particle Synthesis and Characterization

Luminescent Nd-doped $BiVO_4$ particles[1] were prepared by flame spray pyrolysis (FSP). Bismuth nitrate pentahydrate ($Bi(NO_3)_3*5H_2O$)) and stoichiometric amounts of vanadium (ammonium metavanadate, NH_4VO_3) were dissolved separately in a 2:1 volumetric mixture of 2-ethylhexanoic acid and acetic anhydride under magnetic stirring for two hours at 100 °C. The Nd^{3+} is added by dissolving neodymium nitrate hexahydrate ($Nd(NO_3)_3*6H_2O$). The Nd^{3+} concentration was defined as atomic fraction (at%) of the total metal ion concentration resulting in the formula $Bi_{0.99}Nd_{0.01}VO_4$, which has been shown to lead to highest luminescence intensity.[1] The total metal concentration was kept constant at 0.4 M. All chemicals were supplied by Sigma-Aldrich.

The resulting precursor solution was fed at a constant rate (8 ml/min) through a nozzle and dispersed by 3 l/min of oxygen resulting in a fine spray that was ignited and sustained by a surrounding premixed oxygen/methane (1.5/3.2 l/min) flamelet[2]. The particles were collected on a glass microfiber filter (Whatman GF) with the aid of a vacuum pump (Busch Mink MM 1202 AV). The powder X-ray diffraction patterns were recorded with a Bruker D8 advance diffractometer operated at 40 kV and 30 mA with a step size of 0.004°. The crystal sizes were determined using the software Topas 4.2 (Bruker) based on the Rietveld fundamental parameter method. Hydrodynamic sizes were measured by dynamic light scattering using a Zetasizer (Malvern).

Transmission electron microscopy images were recorded via an aberration-corrected, dedicated apparatus (Hitachi-HD2700VD) with a probe corrector (CEOS). Measurements were performed at an acceleration potential of 200 kV (electron gun, cold-field emitter) in ultra-high resolution mode.

Luminescence and thermometry

The NIR fluorescence emission spectra were obtained after excitation with a 750 nm laser diode (CNI Lasers) and recorded with a spectrofluorimeter (FS5, Edinburgh instruments) equipped with a PMT detector (up to 1000 nm) and an InGaAs array (900-1700 nm). The excitation laser light was filtered using a 750 nm bandpass filter (FWHM 40 nm, Thorlabs) and the emission was filtered using 780 nm long-pass filters. For excitation scans, a 150 W Xenon lamp in combination with the built-in monochromator was employed with an excitation bandwidth of 30 nm. Temperature-controlled fluorescence spectra of powders were measured with a heated sample holder (Edinburgh Instruments, SC-28) using the above mentioned spectrofluorimeter. Temperature-controlled fluorescence spectra of aqueous suspensions were recorded on a thermo-electrically cooled cuvette holder (Edinburgh Instruments, SC-25) under magnetic stirring. The aqueous dispersions (0.05 wt%) were achieved through ultrasonication using a water-cooled high intensity cup horn system (VCX500, Sonics Vibracell, Parameters: 95 % amplitude, 28 s ON, 2s OFF) for 5 minutes without any further modification. Fluorescence spectra were recorded with an integration time of 100 ms, if not stated

otherwise, and the reported values and error bars correspond to the average and standard deviation of 5 consecutive measurements.

Temperature measurements

A plexiglass plate of 15 mm thickness with two square (5x5 mm) cavities of 3 mm depth each was placed on a heating plate (Heidolph, MR Hei-Standard). The cavities were filled with a 1:1 mixture of $BiVO_4$:Nd dispersed in water (10 mg/ml) and an aqueous agar solution (1 wt%). Chicken skeletal muscle tissue was placed on top of one of the cavities while the other served as control. During heating, the temperature of the $BiVO_4$:Nd nanothermometers was measured through the chicken tissue using the FIR method under 750 nm excitation using the same filters as above. The laser spot was increased to a circle of 4 cm diameter using a diffuser (Thorlabs, ED1-C20-MD). The laser power was 2 W leading to a power density of 0.16 W/cm^2. The emission spectra were recorded using a portable spectrometer (STS-NIR, Ocean Optics, 100 µm slit), where a separate calibration curve has been performed (using a separate temperature-controlled sample holder, CUV-QPOD, Ocean Optics) to account for the different spectral response of this system with an integration time of 2 seconds without additional optics. The temperatures of the chicken tissue surface and the control $BiVO_4$:Nd were determined by an IR thermal camera (Fluke, Ti110).

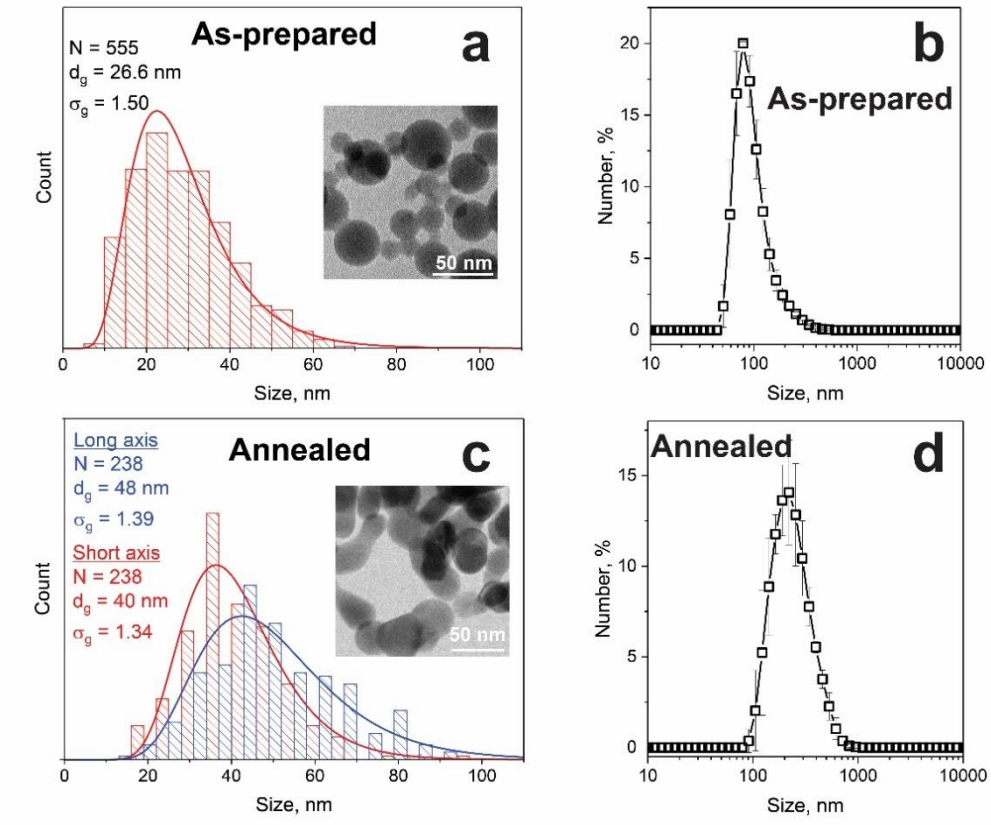

Figure S1: Size distributions of $BiVO_4$:Nd **(a,b)** as-prepared and **(c,d)** after annealing for 2h at 500 °C in air. **(a,c)** Primary particles by counting from TEM images (inset) and **(b,d)** agglomerate distribution determined by DLS.

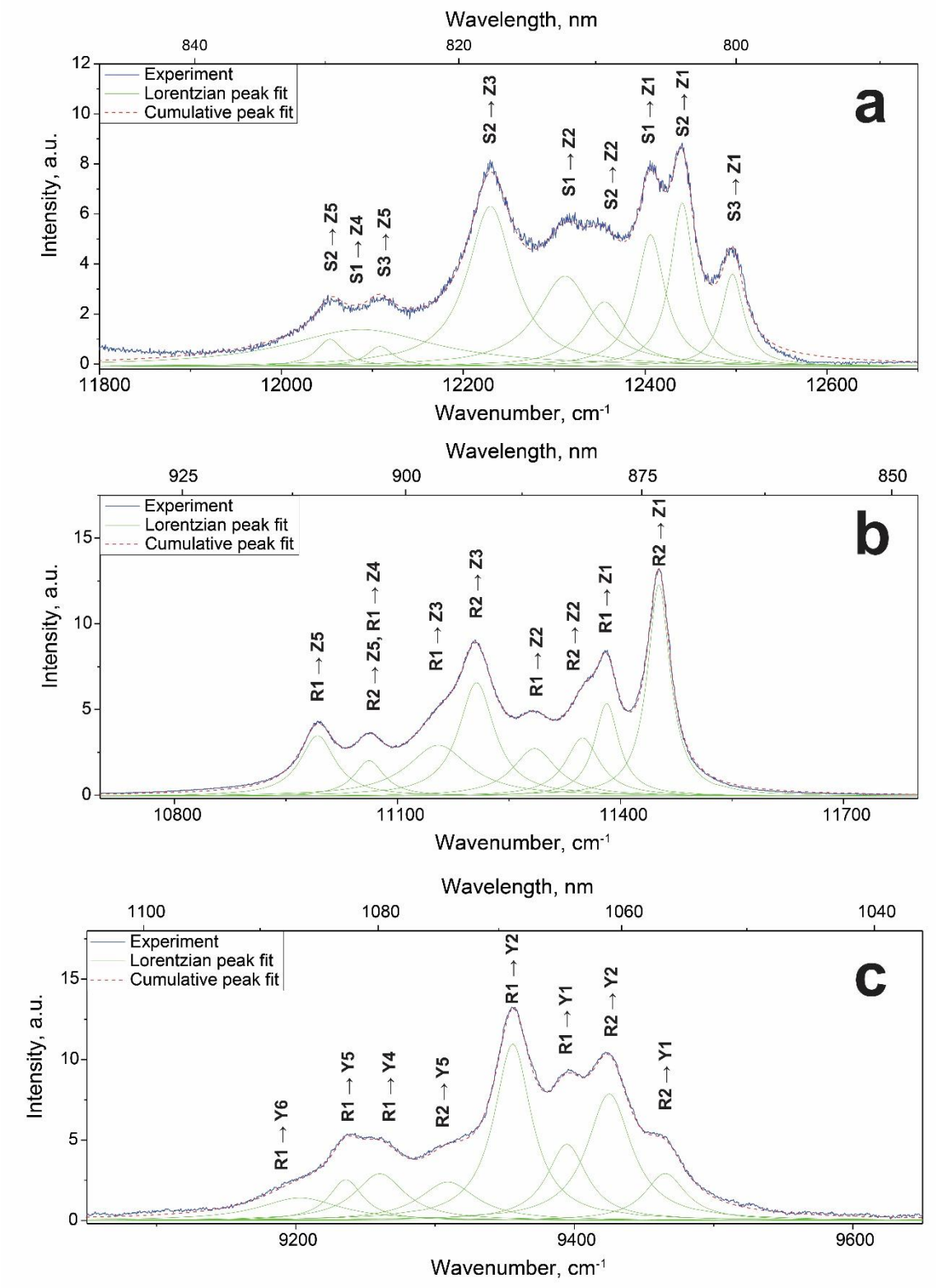

Figure S2: Deconvolution of the emission spectra using Lorentzian peaks for the **a)** $^4F_{5/2} \rightarrow {}^4I_{9/2}$, **b)** $^4F_{3/2} \rightarrow {}^4I_{9/2}$ and **c)** $^4F_{3/2} \rightarrow {}^4I_{11/2}$ transition. Excellent agreement is obtained between the original and reconstructed by deconvolution ones in all three transitions.

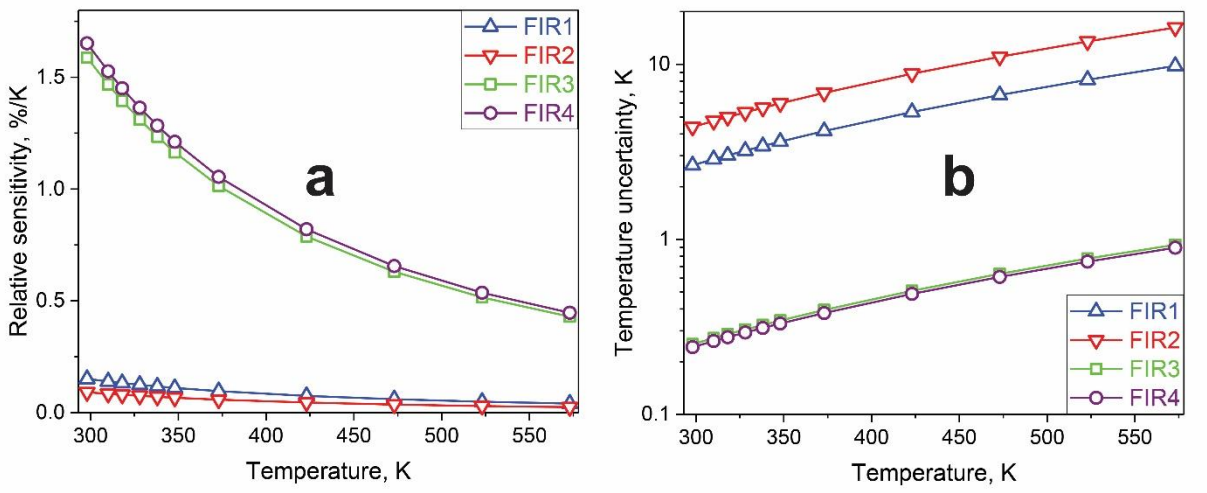

Figure S3: a) Relative thermal sensitivity of Nd-BiVO4 nanothermometers as a function of temperature using the different fluorescence intensity ratios (FIR) and **(b)** temperature uncertainty (from Figure 2).

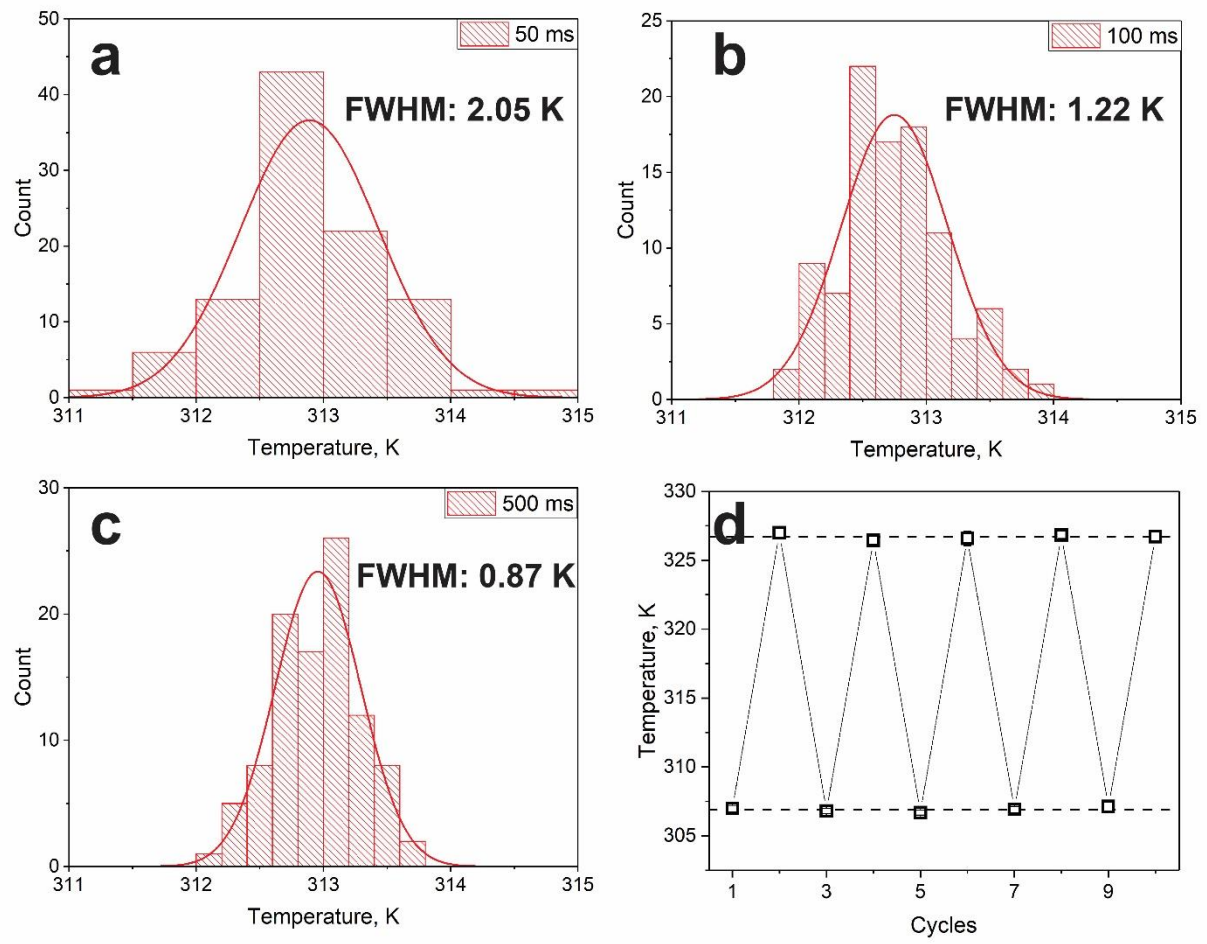

Figure S4: Measured temperature of $BiVO_4$:Nd nanothermometers in aqueous suspension with 100 consecutive scans using **a)** 50, **b)** 100, and **c)** 500 ms integration time. Increasing that time improves the accuracy of nanothermometers. **d)** Ten cycles between 307 and 327 K, showing repeatability[3] higher than 99.6%

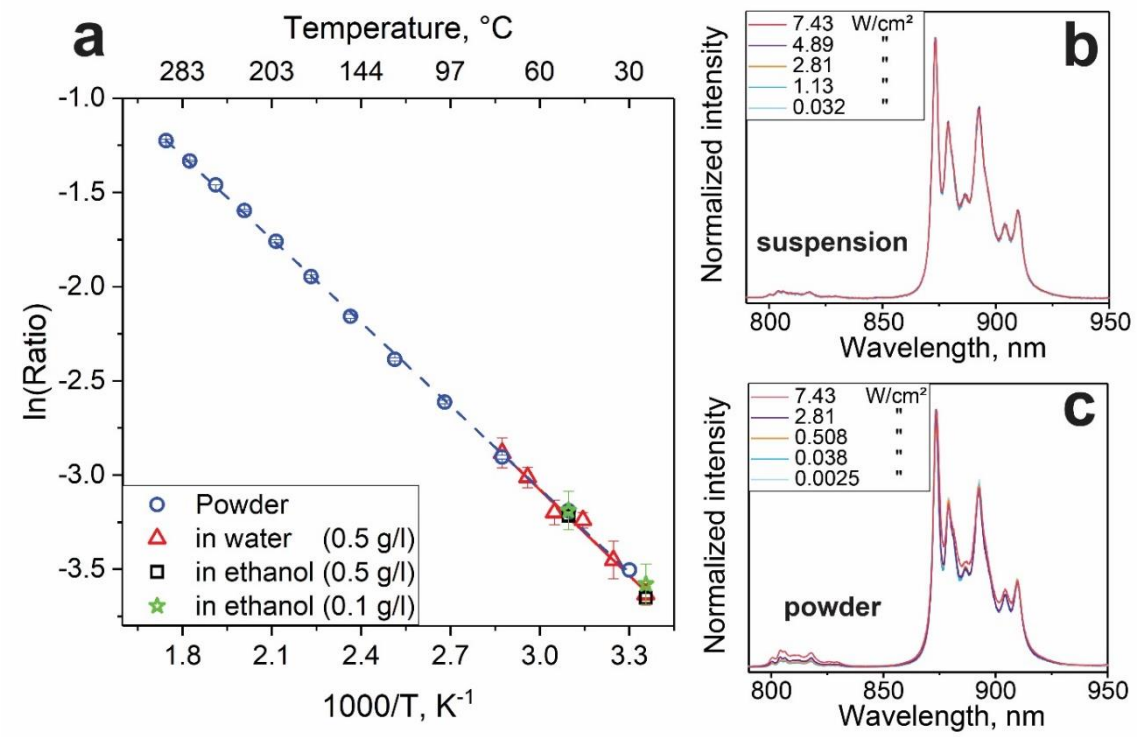

Figure S5: a) Influence of particle environment and concentration on calibration curve, **b)** excitation power on the emission spectra determined in aqueous suspension and **c)** in powder, where excitation densities higher than 2.81 W/cm^2 lead to heating of the particles. Heating does not occur in suspension due to lower particle concentration and better heat dissipation in water resulting in overlapping spectra in (b), in contrast to (c) for high power densities.

Table S1: Measured and calculated energy differences between employed energy levels.

	ΔE measured, cm^{-1}	ΔE calculated[1], cm^{-1}	ΔE calculated[2], cm^{-1}
FIR 1	93 ± 8	390	70
FIR 2	56 ± 6	69	70
FIR 3	980 ± 18	1037	1037
FIR 4	1020 ± 13	2943	1037

[1]: Energy difference based on barycenter[4] of emission peaks

[2]: Energy difference based on contributing thermalized energy levels

Table S2: Performance comparison of Nd^{3+}-containing nanothermometers

Material	λ_{ex} [nm]	FIR[a]		ΔE [cm^{-1}][b]	S_R [%/K]	Source
LaF_3:Nd	808	I_{885}/I_{863}		294	0.10	[5]
$KGd(WO_4)_2$:Nd	808	I_{895}/I_{884}		152	0.11	[6]
$NaYF_4$:Nd	808	I_{870}/I_{863}		93	0.12	[7]
CaF_2:Nd,Gd	573	I_{1058}/I_{867}		2082	0.12	[8]
$Y_3Al_5O_{12}$:Nd	808	I_{945}/I_{938}		79	0.15	[9]
$KGd(WO_4)_2$:Nd	808	I_{1075}/I_{1068}		71	0.15	[6]
YVO_4:Nd	808	I_{888}/I_{879}		108	0.16	[10]
YVO_4:Nd	808	I_{1072}/I_{1064}		109	0.19	[10]
LiP_4O_{12}:Nd	808	I_{871}/I_{866}		66	0.22	[11]
LaF_3:Nd	808	I_{885}/I_{865}		261	0.25	[12]
$LiLaP_4O_{12}$:Nd	808	I_{871}/I_{866}		66	0.31	[13]
LaF_3:Nd	808	I_{863}/I_{861}		27	0.40	[14]
SrF_2:Nd,Gd	573	I_{865}/I_{858}		100	0.56	[15]
Gd_2O_3:Nd	580	$A_{925\text{-}875}/A_{800\text{-}850}$		925	1.25	[4]
$BiVO_4$:Nd	750	$A_{872\text{-}877}/A_{902\text{-}907}$	(FIR 1)	389	0.14	This work
$BiVO_4$:Nd	750	$A_{1059\text{-}1066}/A_{1066\text{-}1071}$	(FIR 2)	56	0.09	"
$BiVO_4$:Nd	750	$A_{790\text{-}840}/A_{840\text{-}945}$	(FIR 3)	1037	1.47	"
$BiVO_4$:Nd	750	$A_{790\text{-}840}/A_{1030\text{-}1130}$	(FIR 4)	2943	1.53	"

[a]: I represents the maximum intensity, A the integrated area of the emission over the given wavelength range

[b]: ΔE calculated from the employed emission centers

References (ESI)

1. F. H. L. Starsich, P. Gschwend, A. Sergeyev, R. Grange and S. E. Pratsinis, *Chem Mater*, 2017, **29**, 8158-8166.
2. L. Madler, W. J. Stark and S. E. Pratsinis, *J Mater Res*, 2002, **17**, 1356-1362.
3. C. D. S. Brites, A. Millan and L. D. Carlos, eds., *Lanthanides in Luminescent Thermometry*, Elsevier, Amsterdam, 2016.
4. S. Balabhadra, M. L. Debasu, C. D. S. Brites, L. A. O. Nunes, O. L. Malta, J. Rocha, M. Bettinelli and L. D. Carlos, *Nanoscale*, 2015, **7**, 17261-17267.
5. U. Rocha, C. Jacinto, W. F. Silva, I. Guedes, A. Benayas, L. M. Maestro, M. A. Elias, E. Bovero, F. C. J. M. van Veggel, J. A. G. Sole and D. Jaque, *ACS Nano*, 2013, **7**, 1188-1199.
6. O. Savchuk, J. J. Carvajal, L. G. De la Cruz, P. Haro-Gonzalez, M. Aguilo and F. Diaz, *J Mater Chem C*, 2016, **4**, 7397-7405.
7. D. Wawrzynczyk, A. Bednarkiewicz, M. Nyk, W. Strek and M. Samoc, *Nanoscale*, 2012, **4**, 6959-6961.
8. P. Cortelletti, C. Facciotti, I. X. Cantarelli, P. Canton, M. Quintanilla, F. Vetrone, A. Speghini and M. Pedroni, *Optical Materials*, 2017, **68**, 29-34.
9. A. Benayas, B. del Rosal, A. Perez-Delgado, K. Santacruz-Gomez, D. Jaque, G. A. Hirata and F. Vetrone, *Adv Opt Mater*, 2015, **3**, 687-694.
10. I. E. Kolesnikov, E. V. Golyeva, M. A. Kurochkin, E. Lahderanta and M. D. Mikhailov, *Sensor Actuat B-Chem*, 2016, **235**, 287-293.

11. L. Marciniak, K. Prorok, A. Bednarkiewicz, A. Kowalczyk, D. Hreniak and W. Strek, *J Lumin*, 2016, **176**, 144-148.
12. E. Carrasco, B. del Rosal, F. Sanz-Rodriguez, A. J. de la Fuente, P. H. Gonzalez, U. Rocha, K. U. Kumar, C. Jacinto, J. G. Sole and D. Jaque, *Adv Funct Mater*, 2015, **25**, 615-626.
13. L. Marciniak, A. Bednarkiewicz, D. Hreniak and W. Strek, *J Mater Chem C*, 2016, **4**, 11284-11290.
14. U. Rocha, C. Jacinto, K. U. Kumar, F. J. Lopez, D. Bravo, J. G. Sole and D. Jaque, *J Lumin*, 2016, **175**, 149-157.
15. M. Pedroni, P. Cortellettia, I. X. Cantarellia, N. Pinna, P. Canton, M. Quintanilla, F. Vetrone and A. Speghini, *Sensors and Actuators B: Chemical*, 2017, **250**, 147-155.